Design and Performance Evaluation of a Vacuum-Based Twist–Bend End-Effector for Automated Mushroom Harvesting with Vision-Based Damage Assessment

Kittiphum Pawikhum , Yanqiu Yang * , Long He , John Pecchia , Paul Heinemann

Posted Date: 10 February 2026

doi: 10.20944/preprints202602.0774.v1

Keywords: automated mushroom harvesting; vacuum-based end-effector; twist–bend detachment; agricultural robotics; damage assessment

 doi:10.20944/preprints202602.0774.v1

Article

Design and Performance Evaluation of a Vacuum-Based Twist–Bend End-Effector for Automated Mushroom Harvesting with Vision-Based Damage Assessment

Kittiphum Pawikhum [1,2], Yanqiu Yang [3,*], Long He [1,2], John Pecchia [4] and Paul Heinemann [1]

[1] Department of Agricultural and Biological Engineering, The Pennsylvania State University, University Park, PA, USA

[2] Fruit Research and Extension Center, The Pennsylvania State University, Biglerville, PA, USA

[3] Department of Animal Science, University of Tennessee, Knoxville, TN, USA

[4] Department of Plant Pathology and Environmental Microbiology, The Pennsylvania State University, University Park, PA, USA

* Correspondence: yyang118@utk.edu; Tel.: +1 (865) 974-9740

Abstract

Manual harvesting of white button mushrooms involves coordinated bending and twisting motions to detach the fruiting body while minimizing surface damage; however, replicating these actions in automated systems remains challenging. In this study, a vacuum-based end-effector that mimics manual twist–bend detachment using a single-point contact was designed and evaluated to reduce mechanical damage. Key detachment parameters, including the friction coefficient (mean 0.62), bending angle (average 5.72°), and twisting torque (average 2.56 N·m), were experimentally analyzed to determine the minimum vacuum pressures required for effective bending and twisting, which were −8.64 ± 2.21 kPa and −8.91 ± 2.45 kPa, respectively, with no significant difference observed between the two motions ($p = 0.51$). A customized vision-based image processing algorithm was developed to quantify postharvest surface damage using a whiteness index (WI). An optimal vacuum pressure of −17.17 kPa was identified, together with a bending angle of 10° and a twisting angle of 90°, balancing high harvesting success with preservation of mushroom quality. The results highlight the influence of end-effector design parameters, including vacuum cup material, contact area, bending direction, and vacuum application duration, on harvesting performance and product marketability, supporting the development of robotic systems for fresh mushroom harvesting.

Keywords: automated mushroom harvesting; vacuum-based end-effector; twist–bend detachment; agricultural robotics; damage assessment

1. Introduction

The specialty crop production industry is a cornerstone of the United States agricultural economy, reflecting its significance in the nation's agricultural landscape. Since the turn of the 21st century, specialty crop production has accounted for over 41% of the U.S. cropland production value [1]. Among these specialty crops, mushrooms are an important economic contributor, generating $1.04 billion for the U.S. economy in the 2022 - 2023 period [2]. White button mushrooms, in particular, have dominated the market, accounting for $945 million in revenue in 2023 [2]. Mushrooms intended for the fresh market are primarily harvested by hand, a labor-intensive process. This challenge led to the development and introduction of mechanical harvesting technologies in the mushroom industry during the late 1970s [3]. Mechanical harvesting allows producers to cover the

 doi:10.20944/preprints202602.0774.v1

same crop area in minutes – a task that would otherwise take days if done manually [4] – but it is not selective and can negatively affect mushroom quality.

The development of automated systems for mushroom harvesting has been a recurring topic in agricultural engineering research [5]. Previous studies have explored the technical feasibility of using automated systems for this purpose, particularly given that mushroom harvesting can account for 15% to 30% of production costs [3]. In 1994, Reed and Tillet developed a robotic mushroom harvesting system that integrated a vision system and a specialized end-effector, achieving 84% location accuracy and a 57% picking success rate. This system emphasized the potential benefits of an effective picking strategy that predicts bend direction and picking order [6]. The original design by Reed was further refined, enabling the robotic harvester to pick approximately 70% of the mushrooms from a container, though high mushroom densities posed challenges. During the experiment, mushrooms touching each other or located on group edges had minimal impact on the system's performance [7]. By 2001, Reed et al. demonstrated the feasibility of robotic mushroom harvesting for the fresh market by incorporating machine vision, image analysis, and delicate handling techniques. Their strategy prioritized picking order and achieved over 80% successful pick attempts during commercial farm trials [8].

Early vision-based mushroom harvesting studies relied on classical image processing methods to identify mushroom size and position using grayscale features, shape tracing, and contour extraction, achieving moderate detection and picking success rates [9]. Subsequent work demonstrated that biological and environmental factors such as mushroom size, orientation, distribution, and flush number significantly influence vision-guided harvester performance [10]. More recent studies have adopted learning-based approaches, including convolutional neural networks and RGB-D sensing, enabling more robust detection, 3D localization, and pose estimation under complex growing conditions [11–14]. These advances in vision sensing have laid the foundation for integrating perception with end-effector design and harvesting strategies in automated mushroom harvesting systems.

Integral to the progress in robotic mushroom harvesting is the design of the end-effector, which directly interacts with the mushrooms. An optimally designed end-effector ensures efficient picking while minimizing damage, thereby preserving the quality and marketability of harvested mushrooms. An end-effector is the tool mounted at the manipulator wrist that directly interacts with the mushroom during harvesting [15]. A primary design requirement is to harvest mushrooms without damaging the cap or inducing post-harvest defects such as bruising or staining [16]. Existing mushroom end-effectors can be broadly categorized into suction-based and gripper-based designs. Suction-based end-effectors typically contact the mushroom cap at a single point, allowing harvesting from any exposed surface, including inclined mushrooms. Prior studies have demonstrated pneumatic suction designs using flexible or pressure-stabilized cups, with reported picking success rates of 90–100% [17–19]. The required vacuum pressure varies widely, ranging from approximately 9 kPa to 172 kPa depending on cup design and harvesting strategy [17,19]. While suction cups simplify grasping and alignment, minor cap damage has been reported several days after harvest in some cases [17].

Gripper-based end-effectors are also widely used, particularly for soft agricultural products, due to their ability to provide secure multi-point contact. These include open grippers with finger-like structures and closed or tubular graspers with internal fingers [20]. In mushroom harvesting, grippers typically grasp the cap from the side rather than the top. Three-finger grippers inspired by the human hand are common and can be soft, rigid–soft hybrid, or fully soft designs [5,21,22]. Soft materials such as PDMS, Ecoflex, and TPU are frequently used at the fingertips to cushion contact forces and reduce cap damage while maintaining high picking success rates [5,22,23]. Commercial systems and research prototypes have demonstrated improved adaptability to mushroom size and shape through finger geometry optimization and asymmetric finger placement [5,22]. Specialized mechanisms, such as drill-assisted end-effectors for harvesting small or densely packed mushrooms during thinning operations, have also been reported [24]. Actuation is commonly achieved using

 doi:10.20944/preprints202602.0774.v1

either electric motors or pneumatic systems, depending on the required force, compliance, and system complexity [24,25].

Several factors, including color, texture, cleanliness, maturity, flush number, and flavor, are used to gauge the quality of button mushrooms. Among these, color is the most critical parameter. It is the first attribute consumers notice, and any discoloration can significantly diminish the mushroom's commercial value [26]. Even a few bruised mushrooms can lead to the downgrading of an entire batch [27]. Consumers often associate brown discoloration, which results from bruising, with inferior quality, leading to reduced demand and lower prices [28]. To evaluate the impact of mechanical damage on mushroom color, the whiteness index (WI) is commonly used as a quantitative measure. Weijn et al. utilized image processing techniques to investigate the effects of mechanical damage on mushroom discoloration, where the WI was employed as a metric to evaluate the efficacy of the designed robotic picking system in comparison to traditional hand picking in preserving mushroom color [29].

This study aimed to design and assess a vacuum-based end-effector capable of replicating the bending and twisting actions involved in manually harvesting white button mushrooms. The research focused on three main objectives: (1) to characterize the mechanical parameters involved in detaching mushrooms—specifically, friction coefficient, bending angle, and twisting torque; (2) to identify the minimum vacuum pressure levels necessary to perform bending and twisting actions without causing visible damage; and (3) to implement an image processing algorithm for calculating WI as a quantitative measure of post-harvest mushroom quality. Through this approach, the study provides a basis for selecting vacuum pressures that ensure high harvesting success while preserving visual quality, thereby supporting the application of robotic harvesting systems in the fresh mushroom market.

2. Materials and Methods

2.1. Experiment Setup and End-Effector Selection

The experiment was conducted at the Penn State Mushroom Research Center (MRC), where mushrooms were spawned and grown in tubs within a controlled environment, as shown in Figure 1a. Typically, mushrooms can be harvested over two to three flushes, but this study focused specifically on the first flush. During stages three to four of the growing process, mushrooms with a cap diameter between 40 - 50 cm were selected for the experiment. The outer vacuum cup had a diameter of 40 cm, with the lip thickness of 5 mm.

(a) (b)

Figure 1. (a) Controlled environment setup at the Penn State Mushroom Research Center (MRC) where mushrooms were grown in tubs for the experiment. (b) Top view of mushrooms growing in close proximity, illustrating the challenge of harvesting mushrooms without damaging adjacent ones.

Manual harvesting involves bending and twisting mushrooms out of the compost, which can be challenging when mushrooms grow close to each other. The vacuum cup was selected as the end-

 doi:10.20944/preprints202602.0774.v1

effector to address this issue because it can grip the mushroom from the top and lift it without damaging the surrounding mushrooms. Figure 1b provides a top view of mushrooms growing in close proximity, illustrating the tight spacing that the vacuum cup must navigate. The vacuum cup was chosen for its ability to effectively grip the mushroom at the top and gently lift it from the compost, even when mushrooms are densely packed with minimal space between them. Precisely controlling vacuum pressure was crucial in this method, as it ensured efficient harvesting while minimizing the risk of damage.

The end-effector was developed to mimic the manual process of picking mushrooms. It serves as the final link between the harvesting system and the mushroom, with the vacuum cup as the key component that directly interacts with the mushroom. The vacuum cup was specifically designed to provide the necessary mechanism for picking, as shown in Figure 2. During the harvesting process, the vacuum cup aligns with the top of the mushroom before gripping it. It then bends the mushroom stem, rotates it, and finally returns to its original position, lifting the mushroom out of the compost. This process is illustrated in Figure 2a–e.

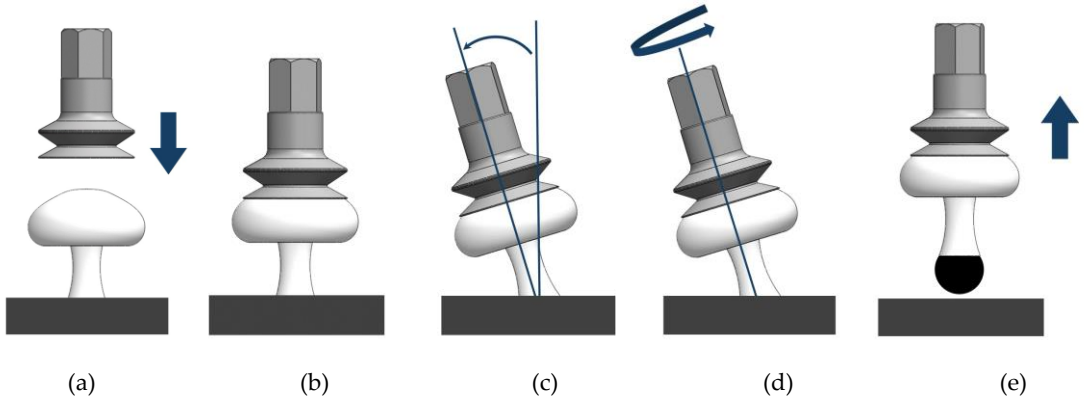

Figure 2. Sequential illustration of the vacuum cup end-effector's process during mushroom harvesting: (a) alignment of the vacuum cup with the top of the mushroom, (b) gripping of the mushroom, (c) bending of the mushroom stem, (d) rotation of the mushroom, and (e) lifting of the mushroom out of the compost.

While the vacuum cup offers significant advantages, such as precision in gripping mushrooms from the top, excessive vacuum pressure can cause bruising and damage [30]. Therefore, determining the minimum vacuum pressure needed to pick the mushroom successfully without causing damage is crucial. This pressure must be just enough to maintain an airtight seal throughout the harvesting process, ensuring that the vacuum cup retains its grip as the mushroom is bent and twisted out of the compost.

Understanding the direction and nature of the forces involved during mushroom harvesting is essential for improving the performance of the vacuum cup as an end-effector. The friction forces generated during bending and twisting exhibit distinct behaviors that directly influence the efficiency and reliability of the harvesting process. Analyzing these forces helps determine the minimum vacuum pressure required to secure the mushroom without causing damage. During bending, the force vector opposes the bending direction, acting against the movement of the mushroom. In contrast, the force moments during twisting act in a different direction, highlighting the unique nature of the forces involved in each process.

2.2. Suction Force Equation for the Vacuum Cup End-Effector

The different behaviors of the forces during the bending and twisting processes can be understood better by examining the fundamental equation that governs the vacuum cup's operation [31]. The suction force F exerted by the vacuum cup on the mushroom is determined by the difference in pressure across the cup's surface and can be expressed as:

 doi:10.20944/preprints202602.0774.v1

$$F = P_{atm} \cdot A_o - P_{suction} \cdot A_i \quad (1)$$

where F represents the upward force exerted by the vacuum cup on the mushroom (N). The atmospheric pressure, P_{atm}, is the pressure exerted by the atmosphere (Pa abs). The area of the outer circle of the suction cup, A_o, is calculated using the equation $A_o = \frac{\pi}{4} D_o^2$, where D_o is the diameter of the suction cup's outer lip (m). The suction pressure inside the cup cavity, $P_{suction}$, is also expressed in Pa (abs). Finally, A_i is the area of the inner circle of suction cup lip, calculated as $A_i = \frac{\pi}{4} D_i^2$, where D_i is the diameter of the suction cup's inner lip circle (m). The configuration and dimensions of the vacuum cup, including both the side and bottom views, are illustrated in Figure 3.

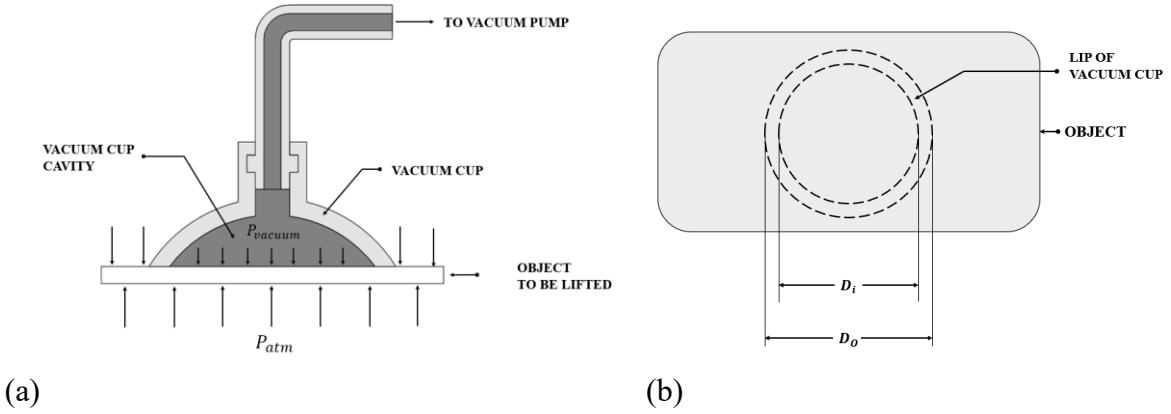

Figure 3. Vacuum cup used to lift an object: (a) Side view, (b) Bottom view.

2.3. Bending Process and Force Analysis

To better understand the mechanical interaction between the vacuum cup and the mushroom during bending, a series of diagrams were developed and analyzed. Figure 4a shows the schematic used to determine the minimum force required for bending the mushroom, where the vacuum cup is subjected to a bending force applied by a robot gripper. This setup illustrates how the vacuum cup deforms and transfers force to the mushroom cap during the bending process. The force interaction between the vacuum cup's surface and the mushroom is further illustrated in Figure 4b, which provides a detailed view of the contact mechanics during bending. The equation used to describe this interaction is derived from principles detailed in Robot Grippers by Monkman et al., ensuring that the calculated force is sufficient to achieve the required bending without damaging the mushroom [32].

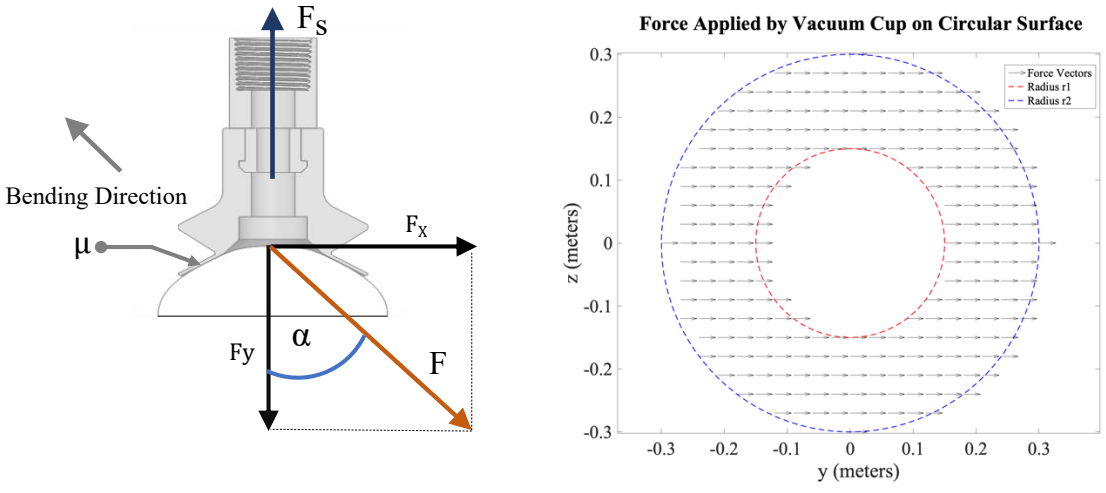

 doi:10.20944/preprints202602.0774.v1

Figure 4. (a) Schematic showing the vacuum cup subjected to a bending force applied by a robot gripper, illustrating the minimum force required for effective bending. (b) Interaction between the vacuum cup and the mushroom cap during the bending process, demonstrating how the vacuum cup deforms and transfers force to the mushroom.

When the vacuum cup bends the mushroom at a bending angle, the force generated by the vacuum cup must be equal to or greater than the force required to displace the mushroom from its position in the compost, as illustrated in Figure 4a. The schematic provides a visual representation of how the vacuum cup interacts with the mushroom cap during the bending process, with the robot gripper applying the necessary force.

The equation governing this interaction is given by:

$$F_s \geq F\left(\cos(\alpha) + \frac{1}{\mu}\cdot\sin(\alpha)\right) \tag{2}$$

where, F_s represents the vacuum-generated force (N), which must be sufficient to overcome the detachment and displacement forces acting on the mushroom during the bending process. The term F denotes the sum of all forces that contribute to the detachment and displacement of the mushroom. The friction coefficient between the vacuum cup and the mushroom cap is represented by μ, and it plays a crucial role in determining the effectiveness of the vacuum cup's grip. Finally, α is the bending angle, which influences the direction and magnitude of the forces involved.

This equation ensures that the force exerted by the vacuum cup is sufficient to overcome the detachment and displacement forces resisting the mushroom's movement during bending. By considering the friction between the vacuum cup and the mushroom, this equation helps determine the minimum force necessary for effective bending without causing the mushroom to detach or shift position.

Converting the force generated by the vacuum cup, as described in Equation (1), into a vacuum pressure equation enhances its utility for controlling the vacuum pressure. This conversion allows the control system to directly regulate the vacuum pressure required to achieve the desired bending force.

$$P_{vacuum} = \frac{P_{atm}\cdot r_2^2}{r_1^2} - \frac{F\left(\cos(\alpha) + \frac{1}{\mu}\cdot\sin(\alpha)\right)}{A_i} \tag{3}$$

where, P_{vacuum} is the vacuum pressure (Pa), which needs to be controlled to achieve the desired force. P_{atm} represents the atmospheric pressure (Pa). The variables r_1 and r_2 denote the inner and outer radii of the vacuum cup, respectively (m). The friction coefficient between the vacuum cup and the mushroom cap is represented by μ, which influences the effectiveness of the vacuum cup's grip. The bending angle is denoted by α, and it affects the direction and magnitude of the forces involved. Finally, A_i is the contact area or the effective area over which the force is distributed (m^2).

Equation (3) provides a direct relationship between the vacuum pressure and the necessary force, making it highly useful for the control system. By adjusting the vacuum pressure according to this equation, the system can ensure that the vacuum cup applies the appropriate force to bend the mushroom effectively while maintaining a secure grip.

2.4. Twisting Process and Torque Analysis

Once the vacuum cup bends the mushroom to a critical angle, the process transitions to twisting the mushroom off the compost, as illustrated in Figure 5a. During this twisting process, the torque generated by the frictional force between the vacuum cup and the mushroom surface plays a crucial role in detaching the mushroom. Figure 5b shows the torque vector that results from this frictional interaction at the contact surface. The torque in this twisting action is also affected by the pressure differential across the cup and the contact area. Building upon the basic pressure equation previously described in Equation (1), where the force exerted by the vacuum cup is determined by the

 doi:10.20944/preprints202602.0774.v1

difference between atmospheric and suction pressures, this concept is extended to calculate the torque necessary for this twisting motion. This calculation ensures that the vacuum cup can effectively twist the mushroom without losing grip, enabling a successful harvest.

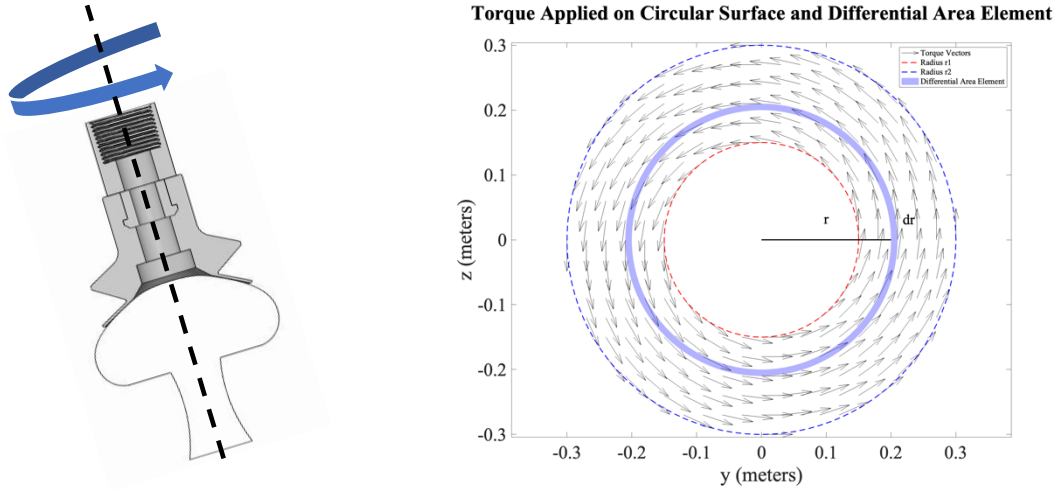

(a) (b)

Figure 5. (a) Schematic illustration of the vacuum cup transitioning from bending to twisting the mushroom off the compost. (b) Torque vector generated by the frictional force at the contact surface during the twisting process.

The contact area between the mushroom and the vacuum cup is modeled as a spherical surface to determine the vacuum pressure required to twist the mushroom out of the compost. The torque generated in this process results from the friction between the vacuum cup surface and the mushroom. The coefficient of friction (μ) between these two materials quantifies the frictional resistance at the interface, which is a critical factor in understanding the interaction during twisting. The normal force (F) exerted on the spherical surface of the vacuum cup is primarily determined by the pressure difference described in Equation (1). The frictional force (f) resisting the relative motion between the vacuum cup and the spherical object during twisting is calculated by multiplying the coefficient of friction (μ) by the normal force (F):

$$f = \mu \times F \tag{4}$$

where, f represents the frictional force at the interface between the vacuum cup and the spherical surface (N). The coefficient of friction (μ) is the measure of resistance between the vacuum cup and the mushroom cap. The normal force (F) is the force exerted by the vacuum cup on the mushroom (N).

To accurately calculate the torque, the contact area of the vacuum cup on the spherical surface must be defined. This area, illustrated in Figure 5b, is characterized by the inner radius (r_1) and outer radius (r_2) of the annular region on the sphere's surface. The inner radius (r_1) and outer radius (r_2) are measured in meters (m) and define the boundaries of the contact area.

The torque contribution from an infinitesimally small element of the contact area is determined by considering a thin strip at a radius r from the center of the sphere, as depicted in Figure 5b. The differential torque (dM_t) exerted by this strip is given by:

$$dM_t = r \times df \tag{5}$$

Substituting the expressions for differential force $df = \mu \times dF$ and the differential normal force $dF = q \times dA$ (where q is the pressure differential and $dA = 2\pi r dr$ is the differential area), the equation becomes:

$$dM_t = r \times \mu \times q \times 2\pi r dr \tag{5}$$

 doi:10.20944/preprints202602.0774.v1

In this equation, dM_t represents the differential torque exerted by the vacuum cup (Nm). The radius r is the distance from the center of the spherical surface to the thin strip of contact (m). The differential frictional force df is the infinitesimal force resisting the twisting motion (N). The pressure differential q across the vacuum cup (Pa) drives the interaction, and dA is the differential area of the thin strip (m^2).

The total torque (M_t) exerted by the vacuum cup over the entire contact area is obtained by integrating the differential torque from r_1 to r_2:

$$M_t = \int_{r_1}^{r_2} 2\pi\mu q r^2 dr = \frac{2\pi\mu q}{3}(r_2^3 - r_1^3) \quad (6)$$

where, M_t is the total torque exerted by the vacuum cup on the spherical surface (Nm). This integral provides the total torque applied by the vacuum cup, which is essential for understanding the forces involved during the twisting motion.

To make the torque equation more applicable for control systems, particularly in robotic applications, it is converted into an expression for vacuum pressure. The vacuum pressure (P_{vacuum}) can be calculated as:

$$P_{vacuum} = P_{atm} - \frac{3M_t}{2\pi\mu(r_2^3 - r_1^3)} \quad (6)$$

This equation directly relates the required vacuum pressure to the torque exerted by the vacuum cup, considering the system's geometric and material properties. This approach provides a comprehensive method for calculating the torque exerted by a vacuum cup on a spherical surface, incorporating factors such as the coefficient of friction, pressure differential, and contact area. The resulting vacuum pressure equation is particularly useful for control systems, where precise adjustments to vacuum pressure are necessary to maintain a secure grip during twisting motions. This approach is crucial in the design of robotic grippers and other automated systems that handle spherical objects in dynamic environments.

2.5. Determination of the Friction Coefficient

The friction coefficient plays a crucial role in both the bending and twisting processes, as it determines how well the vacuum cup adheres to the mushroom cap. Specifically, the friction coefficient is proportional to the traction force and normal force between the two contacting surfaces – in this case, the mushroom cap and the silicone material of the vacuum cup.

An inter-particle mechanics tester [33] was used to accurately determine the friction coefficient. This device measures the friction and adhesion forces by maintaining contact between the silicone and the mushroom while sliding them against each other. During the test, the normal and traction forces were continuously recorded.

To measure the friction coefficient, 80 fresh mushrooms were harvested and cut into uniform cubes with dimensions X (width) and Y (length). Each mushroom cube was securely fastened to a removable particle mount using screws, while silicone was glued to the mount to prevent any movement during the experiment. Figure 6a provides a schematic of the prepared mushroom samples, and Figure 6b illustrates the schematic setup of the silicone used for the test. Figure 6c shows the part of the inter-particle mechanics tester used in the study, with the mushroom and silicone samples mounted in place and ready to slide, specifically designed to measure the friction coefficient between the two materials.

 doi:10.20944/preprints202602.0774.v1

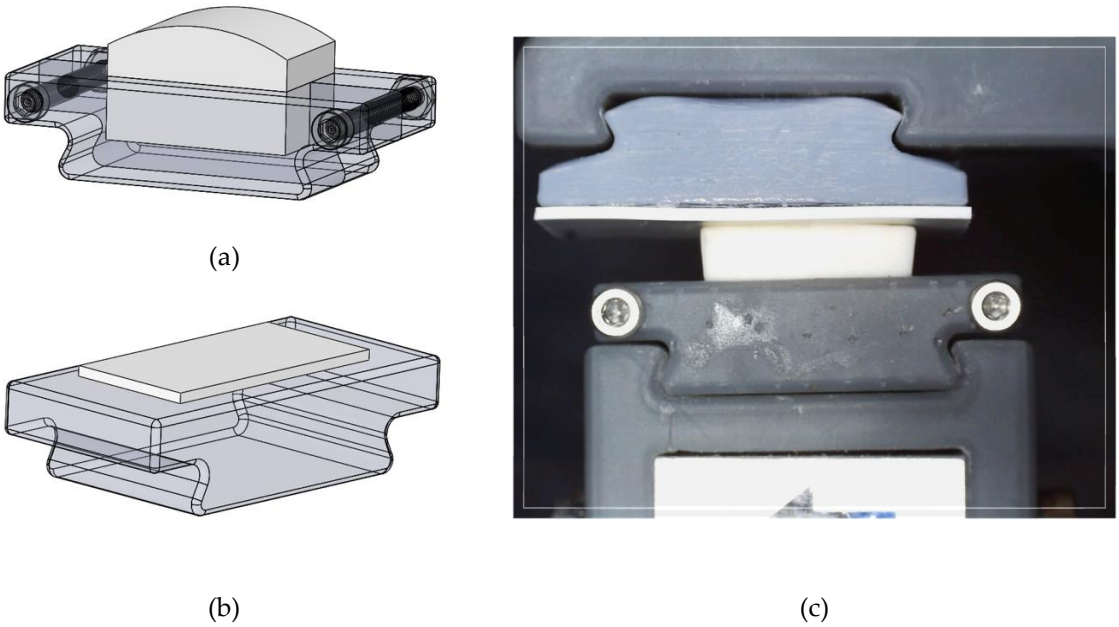

(a) (b) (c)

Figure 6. (a) Schematic of the prepared mushroom samples cut into uniform cubes. (b) Setup of the silicone used for testing friction. (c) The section of the inter-particle mechanics tester where the mushroom and silicone samples are mounted.

2.6. Bending Test and Force Measurement

Bending is the initial picking step before the mushroom is twisted out of the compost. Determining the force and bending angle required to break the mushroom's mycelium is crucial for designing the end-effector. Based on Equation (2), the minimum vacuum pressure needed for bending the mushroom is determined by measuring the bending angle and the critical force necessary to break the mycelium from the compost.

Specialized equipment was required for accurate measurement of the bending angles and the corresponding forces (Figure 7). A load cell was used to measure the bending force with precision. The load cell was positioned at the bottom and attached to the bending finger responsible for bending the mushroom, while the top of the load cell was connected to a linear actuator. The linear actuator's function was to move the bending finger at a consistent rate of 2 mm per minute, ensuring reliable measurement of the bending force.

The bending angle α was calculated using the following formula:

$$\alpha = \arctan\left(\frac{X}{H}\right) \tag{7}$$

where, α represents the bending angle, X is the horizontal displacement of the bending finger (m), and the height H (m) is the vertical distance from the point where the bending finger contacts the mushroom to the bottom of the mushroom. Since the bottom of the mushroom is embedded in the compost, H was measured after the experiment.

 doi:10.20944/preprints202602.0774.v1

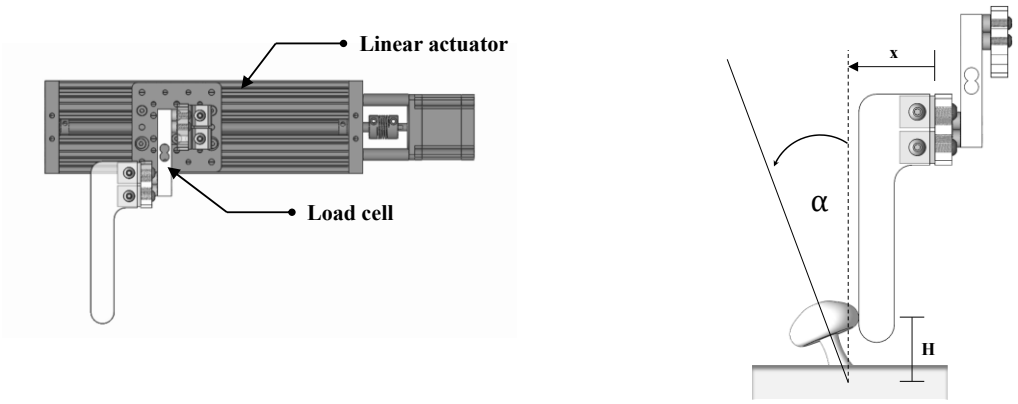

(a) (b)

Figure 7. Schematic of the mushroom bending force measurement system. (a) Position of the load cell, bending finger, and linear actuator used to measure the bending force. (b) Bending process with displacement X and height H indicated, used to calculate the bending angle α.

Throughout the experiment (Figure 8), both the bending force and the bending angle were continuously monitored until the mushroom cap was pressed against the compost. The critical force, which is the force required to break the mycelium, was then converted into the necessary pressure to determine the minimum pressure needed for the bending process. Figure 8a shows the experimental setup in the real environment, while Figure 8b illustrates the height measurement between the point where the bending finger makes contact with the mushroom and the base of the mushroom after the bending process. These measurements of minimum pressure and bending angle are crucial for designing an effective end-effector for the mushroom-picking process.

(a) (b)

Figure 8. Experiment setup of the mushroom bending force measurement system: (a) Experimental setup in a real environment, showing the bending force applied to the mushroom until the cap touches the compost. (b) Height measurement between the point of contact with the bending finger and the mushroom base after the bending process.

2.7. Twisting Test and Torque Measurement

When harvesting white button mushrooms, twisting after bending is crucial for ensuring that the mycelium remains within the compost, allowing for subsequent flushes. Without twisting, directly lifting the mushroom after bending can pull the mycelium out, negatively affecting future productivity. To determine the minimum pressure required for twisting mushrooms out of the substrate, it is necessary to accurately measure the torque applied during the twisting process after bending the mushroom to a critical angle. As shown in Figure 9, the torque measurement system

 doi:10.20944/preprints202602.0774.v1

consists of four main components, each playing a vital role in ensuring precise control and measurement.

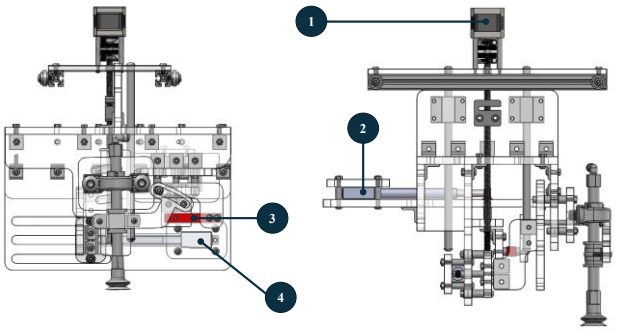

Figure 9. Schematic of the mushroom twisting torque measurement system. The system includes four key components: (1) a stepper motor with a lead screw for vacuum cup positioning, (2) a linear actuator for executing the twisting motion, (3) a load cell for real-time torque measurement, and (4) a linear actuator for controlled bending. This setup ensures precise measurement of the torque and angle needed for effective mushroom harvesting without damaging the crop or mycelium.

The first component, a stepper motor (number 1), is connected to a lead screw, enabling the vacuum cup to move up and down to securely grip the mushroom cap before bending and twisting. The second component, a linear actuator (number 4), manages the bending motion by pushing a pin along a slot, bending the mushroom to a predetermined critical angle and setting a consistent starting point for twisting. The third component is a load cell (number 3) integrated with a second linear actuator (number 2), which measures the torque generated during the twisting process, providing real-time data to determine the minimum pressure required for effective harvesting. This second linear actuator (number 2) is designed to perform the twisting action, rotating the mushroom up to 90° to ensure precise control over the applied force, allowing the mushroom to be detached without damaging its structure or the surrounding mycelium. This integrated system enables accurate measurement of the torque and angle needed for twisting, which is critical for designing an effective end-effector for mushroom harvesting.

The mushroom twisting torque measurement system utilizes a vacuum to grip the mushroom securely, ensuring it does not slip during the twisting process. The operational steps of the system are illustrated in Figure 10. Initially, the system is manually positioned above the mushroom. The stepper motor then lowers the system, allowing the vacuum cup to grip the mushroom firmly. Once the mushroom is securely gripped, the first linear actuator engages, pushing a pin attached to the vacuum cup to bend the mushroom to a predetermined critical angle. After a 5 s pause, the second linear actuator activates, twisting the mushroom. During this twisting process, the load cell continuously records the force applied from 0 to 90° of rotation, as depicted in Figure 10 a-d.

 doi:10.20944/preprints202602.0774.v1

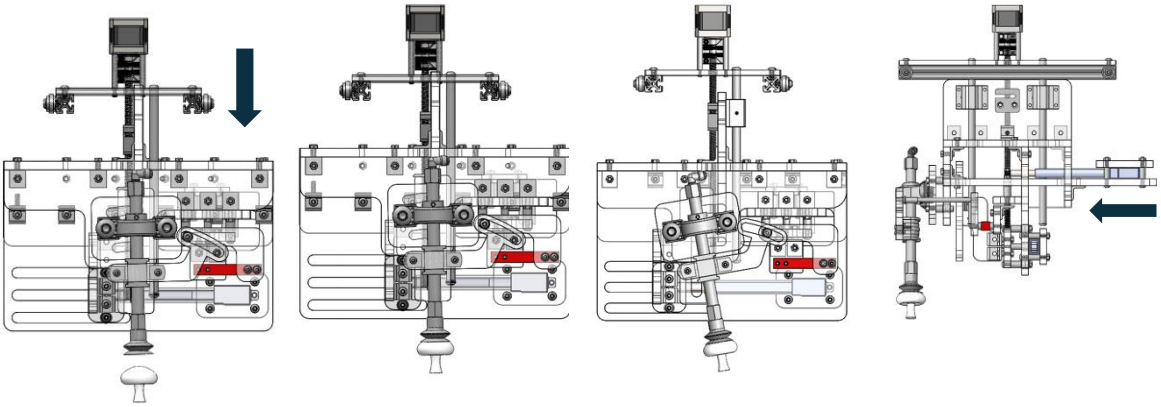

(a) (b) (c) (d)

Figure 10. Operational steps of the mushroom twisting torque measurement system: (a) positioning above the mushroom, (b) lowering of the vacuum cup to grip the mushroom, (c) bending of the mushroom to the critical angle, (d) twisting of the mushroom, with the load cell recording the force applied.

The minimum vacuum pressure required for twisting the mushroom is determined by calculating the torque, which is essential for ensuring that the mushroom is securely gripped without damage. The force measured during the experiment, which is the force used to rotate the vacuum cup, is converted to torque using the equation $M_t = r \times F$, where Mt represents the total torque, r is the distance from the pivot point to the point where the force is applied, and F is the force exerted to rotate the vacuum cup during the twisting process. This conversion is schematically illustrated in Figure 11a. The torque required to rotate the vacuum cup without a mushroom was first measured for calibration purposes. The data collected with the mushroom was then adjusted by subtracting the torque measured without the mushroom. This corrected torque data was used to calculate the minimum vacuum pressure needed for designing an end-effector that effectively combines the bending and twisting processes.

Throughout the twisting process, the total torque and the twisting angle were recorded, and this information was then used to design the end-effector, ensuring it can harvest mushrooms without causing damage. Figure 11b shows the actual setup of the system installed and tested in a real-world environment, demonstrating how the components work together to achieve precise and reliable measurements.

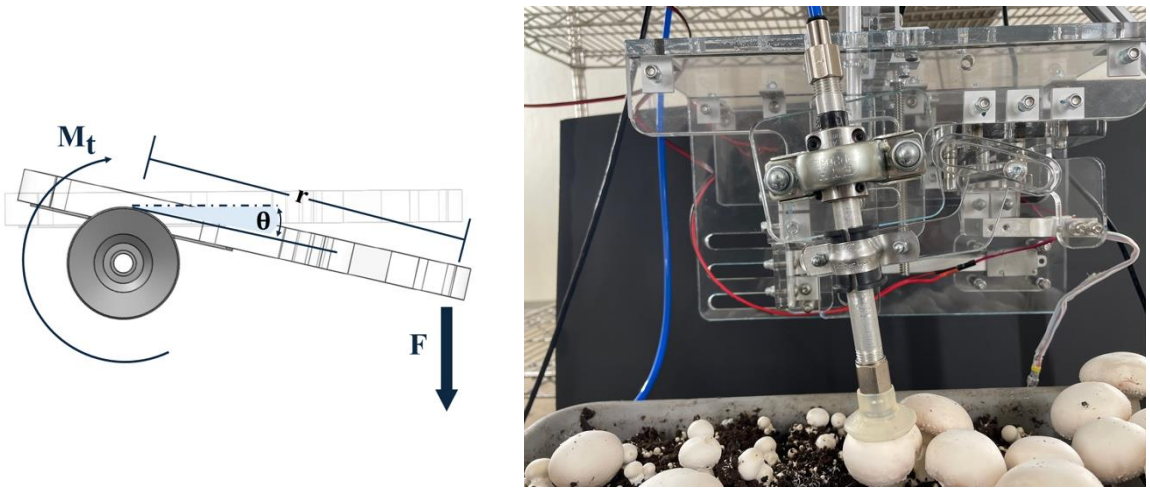

(a) (b)

 doi:10.20944/preprints202602.0774.v1

Figure 11. (a) Schematic illustration of the torque calculation process, showing the relationship between the applied force, pivot point, and resulting torque. (b) The actual setup of the mushroom twisting torque measurement system installed and tested in a real-world environment.

2.8. Development of the End-Effector Based on Bending and Twisting Tests

The design of the end-effector for the automatic harvesting of mushrooms is based on the findings from the bending and twisting experiments described in the previous section. This end-effector mimics the manual process of picking mushrooms by combining the actions of bending and twisting. The bending test provided crucial information for determining the optimal bending angle, while the twisting test informed the design of the twisting mechanism. Additionally, the vacuum pressure data obtained from these experiments was used to control the vacuum pressure in the end-effector.

The end-effector comprises three main components that worked together to achieve the combined bending and twisting action, as shown in Figure 12. First, the vacuum cup was responsible for securely gripping the mushroom. Second, a stepper motor was used to execute the twisting motion of the mushroom. Finally, a pneumatic cylinder was employed to bend the mushroom to the desired angle. Together, these components ensured that the mushroom is harvested efficiently and without damage.

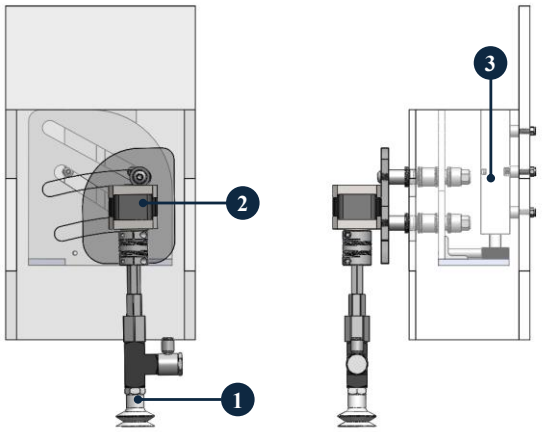

Figure 12. Main components of the mushroom harvesting end-effector. The end-effector includes: (1) a vacuum cup for gripping, (2) a stepper motor for twisting, and (3) a pneumatic cylinder for bending the mushroom.

The end-effector was designed with two primary mechanisms that worked sequentially to pick mushrooms: bending and twisting. The bending mechanism operated through a pneumatic cylinder attached to a slot, which pushed a pin to guide the twisting mechanism, bending the mushroom to the desired angle. When the pneumatic cylinder extended, it moved the pin along the slot, allowing the twisting mechanism to achieve the critical bending angle necessary for proper mushroom harvesting, as shown in Figures 13a and 13b. Following this, the twisting mechanism, driven by a stepper motor, rotated the mushroom and completed the harvesting process. Figure 13c illustrates how the stepper motor twists the mushroom, ensuring it was detached from the substrate without causing damage.

 doi:10.20944/preprints202602.0774.v1

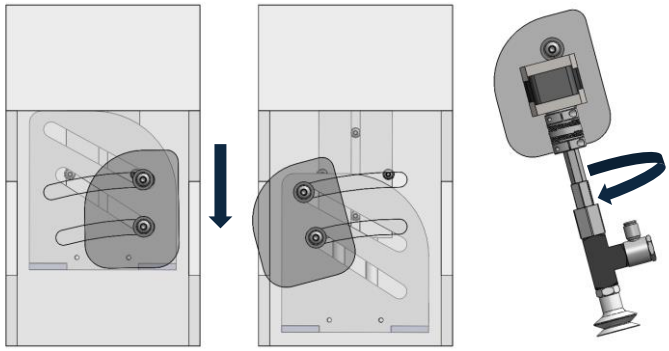

Figure 13. Operation of the mushroom harvesting end-effector: (a) the pneumatic cylinder initiates the bending mechanism, (b) the mushroom is bent to the desired angle, (c) the stepper motor twists the mushroom to complete the harvest.

The mushroom harvester's end-effector was carefully designed and constructed based on experiments that determined the necessary bending angles and twisting torque. Figure 14 (steps a-g) illustrates each stage of the harvesting process, from aligning the end-effector with the mushroom to lifting it out of the compost. The harvesting process began with the end-effector aligning directly above the mushroom (Figure 14a). Next, the end-effector moved forward to grip the mushroom securely (Figure 14b). Once gripped, a pneumatic cylinder pushed a pin to bend the mushroom stem by 10° (Figure 14c). Simultaneously, a stepper motor rotated the end-effector 90°, applying a twisting motion to detach the mushroom (Figure 14d). After detachment, the stepper motor reset to its original position, undoing the 90° twist (Figure 14e). The pneumatic cylinder then retracted the pin, releasing the bend in the mushroom stem (Figure 14f). Finally, a linear actuator lifted the mushroom out of the compost, completing the harvesting process (Figure 14g).

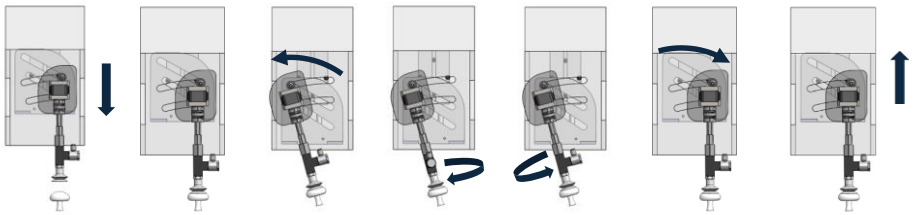

Figure 14. Stages of the mushroom harvesting process: (a) alignment of the end-effector above the mushroom, (b) secure gripping of the mushroom, (c) bending the mushroom stem by 10°, (d) twisting the mushroom by 90° to detach it, (e) resetting the twist, (f) releasing the bend, (g) lifting the mushroom out of the compost.

2.9. Whiteness Index Calculation

The success of the mushroom industry relies on delivering high-quality mushrooms to the fresh market, where the whiteness index (WI) is a key criterion for evaluating the quality of white button mushrooms. Whiteness is a crucial indicator of freshness and consumer appeal. Currently, mushrooms are harvested by hand. The effectiveness of the vacuum cup end-effector, tested under varying vacuum gauge pressures of -5 kPa, -10 kPa, -15 kPa, and -20 kPa, was compared with the current hand-picking practice. For each treatment, 50 randomly selected post-harvest mushrooms were used to measure the WI.

After harvesting, the mushrooms from each treatment group had their stems cut to a uniform length of 3/8 in. (9.525 mm) from the mushroom cap. Each mushroom was gently placed on a

 doi:10.20944/preprints202602.0774.v1

numbered blackboard for tracking purposes and then placed in a container to protect the caps during storage in a cooler room maintained at 4°C, as shown in Figure 15.

(a) (b)

Figure 15. Mushroom labeling and storage process in a blackboard segmented container after harvesting and stem trimming for Whiteness Index evaluation.

The process for measuring the WI is illustrated in Figure 16. During image collection, the mushrooms were placed in a black box designed to maintain consistent illumination conditions, and images were captured from the top using a standardized setup. These images were then loaded into MATLAB (R2023b; MathWorks Inc., Natick, MA, United States) for processing. Four points on the white reference area and four points on the mushroom surface were manually selected to define and crop rectangular regions of interest (ROIs) for further analysis. The white reference region was converted from the sRGB color space to the CIELAB color space, and the mean lightness (L*) value was calculated, where L* represents lightness, a* represents the red–green chromaticity component, and b* represents the yellow–blue chromaticity component. The L* values across the entire image were adjusted to align with a reference L* value of 100, corresponding to ideal white, to standardize the lightness. The corrected mushroom region was then extracted, converted to grayscale, and analyzed using a threshold to segment the mushroom from the background. The largest contour was detected and used to create a binary mask isolating the mushroom. The masked mushroom region was then converted to the CIELAB color space, and the WI was calculated for each pixel within the masked area using equation 8:

$$WI = L^* - 3b^* + 3a^* \quad (8)$$

Following the initial image capture, the mushrooms were stored in the cooler room, and every 24 hours, they were returned to the black box for additional image captures to measure the WI over 8 days. The mean WI was calculated and reported to provide a standardized assessment of the mushroom's visual appearance. The comparison of WI between robot and hand-picking methods was conducted to determine whether the robot-harvested mushrooms met the quality standards necessary for the fresh market. The results indicated that the differences in whiteness were within acceptable limits, confirming the viability of the robot-picking method for maintaining the quality expected by consumers.

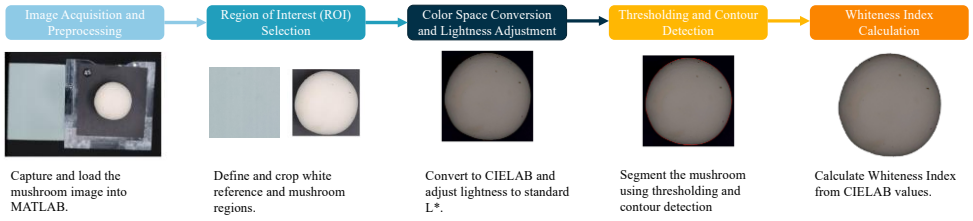

Figure 16. Process for measuring the whiteness index (WI): (a) placement of mushrooms in a black box for standardized imaging, (b) image processing steps in MATLAB, including selection of regions of interest, conversion to CIELAB color space, and calculation of the Whiteness Index.

 doi:10.20944/preprints202602.0774.v1

3. Results and Discussion

3.1. Friction Coefficient

The friction coefficient between the mushroom surface and the silicone material of the vacuum cup was measured for 80 fresh mushroom samples. An example of the results is shown in Figure 17a, where the linear regression slope for this pair of mushroom and silicone represents the friction coefficient. The mean friction coefficient for all samples was 0.621, with a standard deviation of 0.193. The measured friction coefficients ranged from 0.044 to 1.2, with most values clustering around the mean, as shown in Figure 17b.

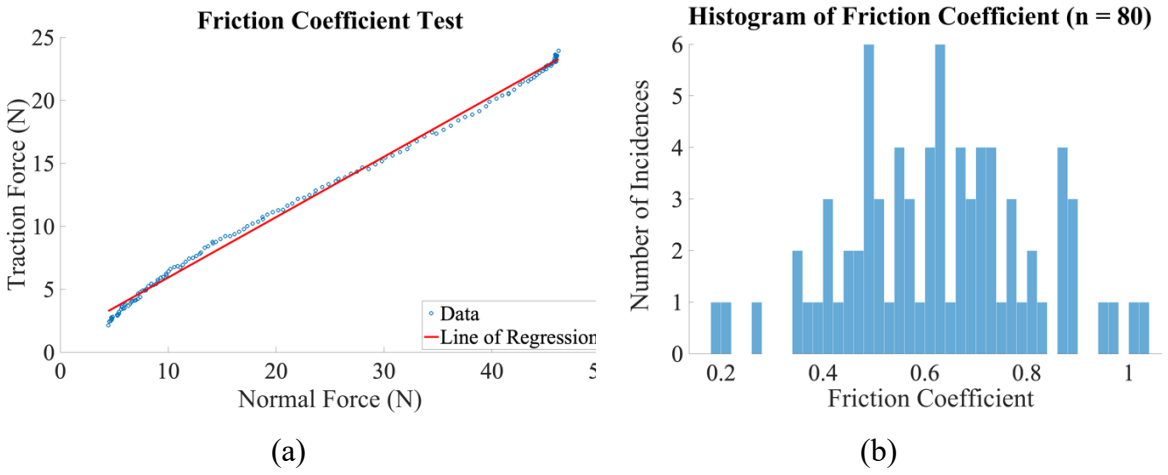

Figure 17. Friction coefficient: (a) Linear regression slope representing the friction coefficient between a mushroom sample and the silicone material of the vacuum cup, (b) Distribution of measured friction coefficient for all samples, ranging from 0.044 to 1.2, with most values clustering around the mean of 0.621 (±0.193).

The measured friction coefficients fall within the expected range for interactions between organic materials and silicone surfaces. A higher friction coefficient generally correlates with a firmer grip, which helps prevent slippage during mushroom harvesting. However, our research also highlights the potential risks of excessive friction, which could increase the risk of damaging the mushroom cap. This understanding can guide the safe and effective use of vacuum pressure in mushroom harvesting, providing reassurance and confidence.

The results suggest that the vacuum pressure should be calibrated according to the measured friction coefficient to achieve an optimal grip without damaging the mushroom. For instance, a friction coefficient closer to 1.2 may allow for lower vacuum pressure, while a coefficient near 0.044 might require a higher pressure to maintain an effective seal. Thus, the results provide clear guidelines for practical application.

The design and control of the vacuum cup were based on the minimum friction coefficient observed to ensure sufficient vacuum pressure for picking mushrooms. This value was calculated using Equation (2) for bending and Equation (3) for twisting. The friction coefficient values were assessed for normal distribution using the Kolmogorov-Smirnov test (P-Value = 0.954), confirming that they follow a normal distribution. This analysis recommends a friction coefficient of 0.235 for the design to provide adequate force. This value represents the mean minus two standard deviations, corresponding to a 95% confidence interval, ensuring that the vacuum cup operates effectively within the lowest 2.5% of friction coefficients observed, thereby minimizing the risk of damage while maintaining an adequate grip.

3.2. Bending Test Results

The bending angle and the force required to bend mushrooms were recorded for a total of 80 mushrooms. The results of these experiments are illustrated in Figure 18, which shows the force-

 doi:10.20944/preprints202602.0774.v1

bending angle relationship for two example cases. In the first case (mushroom 1), the force increased dramatically as the finger began to push the mushroom, followed by a gradual decrease. When the bending angle reached 12 °, a sudden drop in force indicated the critical bending point. In contrast, mushroom 2 showed a sudden drop in force at a bending angle of just 5°.

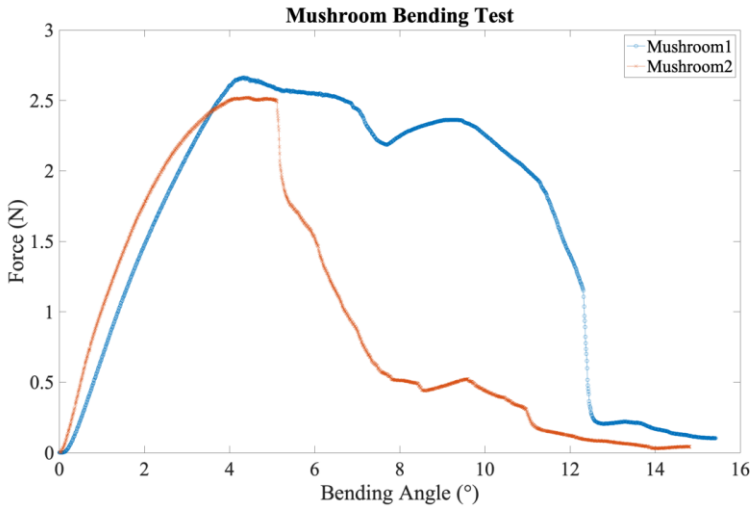

Figure 18. Force-bending angle relationship: Example cases showing the force required to bend two mushroom samples. For mushroom 1, the force increases sharply, followed by a gradual decrease, with a critical bending point at 12°. For mushroom 2, the critical bending point occurs at 5°, indicated by a sudden drop in force.

The data collected from these experiments revealed that the critical bending angle, where the force suddenly dropped, had an average value of 5.72° with a standard deviation of 1.75°. The average bending force recorded was 2.59 N, with a standard deviation of 1.45 N. This bending force was then converted to the required vacuum pressure (P_{vacuum}) using Equation (2). For control purposes, P_{vacuum} was further converted to P_{gauge}, resulting in an average value of -8.64 kPa with a standard deviation of 2.21 kPa. These findings have significant implications for vacuum pressure control, enhancing understandings of the relationship between force, bending angle, and vacuum pressure.

It is important to note that not all mushrooms exhibited a force drop during the bending process. The length of the mushroom stem proved to be a critical factor. Mushrooms with shorter stems had their caps come into contact with the substrate before the mycelium broke, which increased the bending force and caused potential damage to the mushroom. This also resulted in dirtier mushrooms during picking. Based on these findings, it is recommended that the end-effector be designed to incorporate a bending angle of 10° to optimize the harvesting process and minimize damage.

3.3. Twisting Test Results

The behavior of mushrooms during the twisting process differs significantly from that observed during bending. The graph below illustrates an example of the torque applied during the twisting test (Figure 19). As the mushroom was twisted, the torque gradually increased, with some fluctuations throughout the process. In this particular case, the torque peaked at its maximum value when the mushroom was twisted to 60°. After reaching this peak, the torque remained relatively stable around 1.75 Nm as the twisting angle increased to 90°, which is the maximum twisting angle measurable by the system developed for this test.

 doi:10.20944/preprints202602.0774.v1

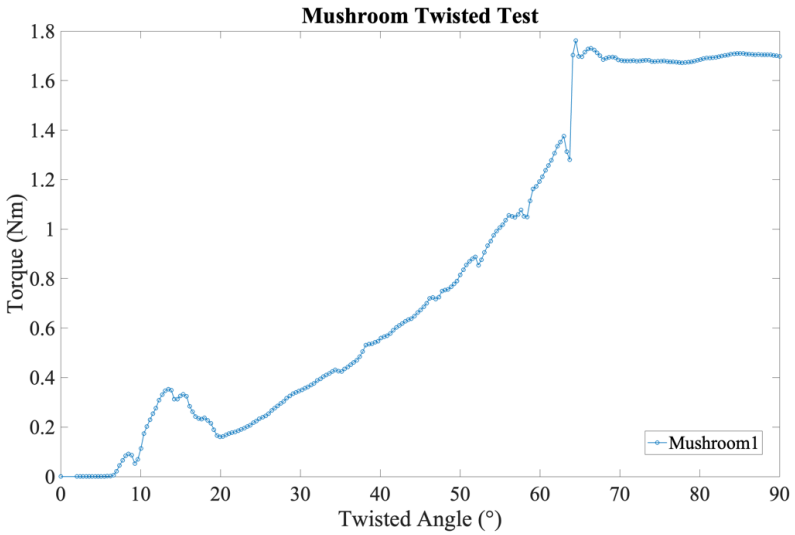

Figure 19. Torque-twisting angle relationship: The graph shows the torque applied during the twisting test for a mushroom sample. The torque gradually increases, peaking at 1.78 Nm when the mushroom reaches a 60° twist, and remains stable as the twisting angle increases to the maximum measurable angle of 90°.

Data were collected from 60 mushrooms, and the results showed an average torque of 2.56 Nm with a standard deviation of 0.74 Nm. This torque was then converted to the corresponding vacuum pressure using Equation (3). For control purposes, the vacuum pressure was further converted to gauge pressure, resulting in an average value of -8.91 kPa with a standard deviation of 2.45 kPa.

The twisting experiment revealed that the torque required to twist the mushroom does not consistently decrease after reaching a 90° twist. Instead, the torque either remains stable, continues to increase in some scenarios, or drops slightly, allowing for capturing the maximum torque value, which is crucial for calculating the necessary vacuum pressure for the end-effector. Based on these results, it is recommended that the end-effector be designed to twist the mushroom up to 90° after the initial bending. This recommendation is grounded in the capabilities of the current twisting torque measurement system, which effectively collects data between 0 and 90° of twist.

However, it is essential to acknowledge the limitations of the current system. While it successfully captures the maximum torque within the 90° range, it does not measure torque beyond this point. Future work should enhance the twisting torque measurement system to capture data over a 360° twist, improving the accuracy and effectiveness of the designed end-effector. Enhancing the measurement system would provide a more comprehensive understanding of torque behavior throughout the twisting process, ultimately leading to a more optimized design for the end-effector.

3.4. Comparison of the Minimum Vacuum Pressure for Bending and Twisting

The minimum pressure gauge values from the bending and twisting experiments were compared to determine the optimal minimum pressure for controlling the end-effector. The higher pressure between the two experiments was selected to ensure the vacuum cup securely grips the mushroom throughout the harvesting process. The pressure data from the bending experiment followed a normal distribution, as confirmed by the Kolmogorov-Smirnov test (P-Value = 0.22). Similarly, the pressure data from the twisting experiment also followed a normal distribution (P-Value = 0.61). A comprehensive comparison of the mean pressures from both experiments was conducted using an independent samples t-test, resulting in a P-Value of 0.51, indicating no significant difference between the minimum pressures required for bending and twisting. Figure 20 presents a boxplot comparing the minimum vacuum pressures from the bending and twisting experiments, illustrating that the pressures required for both processes are statistically similar.

 doi:10.20944/preprints202602.0774.v1

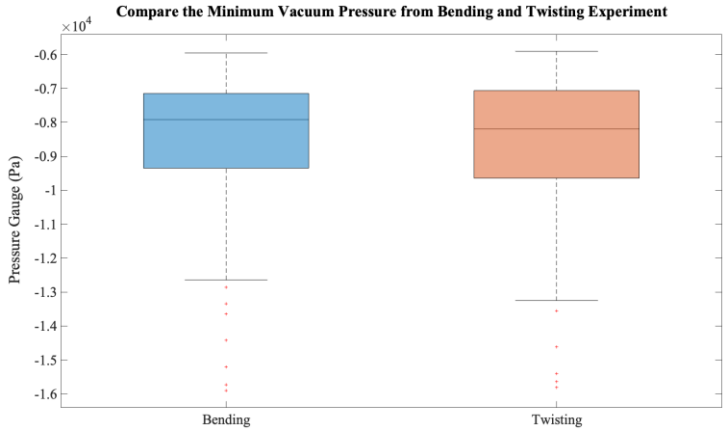

Figure 20. Comparison of minimum vacuum pressures: Boxplot showing the minimum vacuum pressures required for bending and twisting experiments. Statistical analysis indicates no significant difference between the pressures for both processes, as evidenced by the similar pressure values.

3.5. Final Design and Success Rate of the End-Effector Prototype

The mushroom harvester's end-effector was carefully designed and constructed based on experiments that determined the necessary bending angles and torque. Figure 21 (steps a-g) illustrates each stage of the harvesting process, from aligning the end-effector with the mushroom to lifting it out of the compost. The harvesting process begins with the end-effector aligning directly above the mushroom (Figure 21a). Next, the end-effector moves forward to grip the mushroom securely (Figure 21b). Once gripped, a pneumatic cylinder pushes a pin to bend the mushroom stem by 10° (Figure 21c). Simultaneously, a stepper motor rotates the end-effector 90°, applying a twisting motion to detach the mushroom (Figure 21d). After detachment, the stepper motor resets to its original position, undoing the 90° twist (Figure 21e). The pneumatic cylinder then retracts the pin, releasing the bend in the mushroom stem (Figure 21f). Finally, a linear actuator lifts the mushroom out of the compost, completing the harvesting process (Figure 21g).

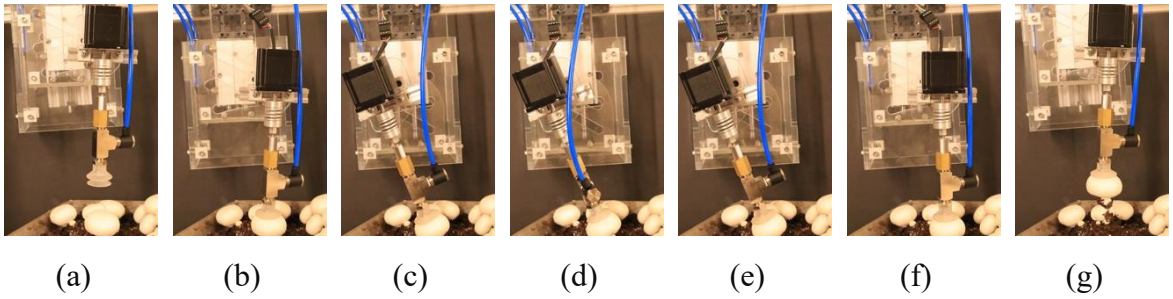

Figure 21. Sequential stages of the mushroom harvesting process: (a) The end-effector aligns directly above the mushroom. (b) The end-effector moves forward to securely grip the mushroom. (c) A pneumatic cylinder bends the mushroom stem by 10o. (d) A stepper motor rotates the end-effector 90o to apply a twisting motion for detachment. (e) The stepper motor resets to undo the twist. (f) The pneumatic cylinder retracts, releasing the bent stem. (g) A linear actuator lifts the mushroom out of the compost, completing the harvest.

The minimum vacuum pressure was carefully applied to the vacuum cup during the picking process to optimize the balance between success rate and mushroom integrity. As detailed in Table 1, the end-effector's success rate for picking mushrooms was tested at various pressure levels. The experiment began with a minimum pressure of -5 kPa, derived from the bending and twisting experiments, and then gradually increased to -10 kPa, -15 kPa, and -20 kPa.

 doi:10.20944/preprints202602.0774.v1

Table 1. Success rate of mushroom picking at various vacuum pressure levels.

P-vacuum Gauge (kPa)	Success Rate (%) n = 80
-5	73
-10	83
-15	92
-20	97

In each trial, 80 mushrooms were randomly picked. The results showed a clear trend: as vacuum pressure increased, so did the success rate. At -5 kPa, the success rate was 73%. This rate improved to 83% at -10 kPa, 92% at -15 kPa, and reached 97% at -20 kPa.

However, several factors can contribute to the failure of the picking process. One major factor is the direction in which the end-effector bends the mushroom. For optimal success, the mushroom should be bent towards an open space, without any surrounding mushrooms that might interfere. Bending in a direction where mushrooms are clustered together can cause the vacuum cup to leak, resulting in process failure.

Although higher pressure generally improves the success rate, a goal of this study is to ensure that the mushrooms remain suitable for the fresh market after picking. At higher pressures, particularly at -20 kPa, the vacuum cup began to leave noticeable damage on the mushroom caps. Fifty mushrooms from each pressure treatment were collected, and their whiteness index – a key factor in consumer perception – was measured to assess the impact on quality.

3.6. Whiteness Index Evaluation

The success rate of mushroom harvesting is a crucial metric for evaluating the performance of an end-effector, but it is not the only factor. The whiteness index (WI) is also used as an evaluation criterion to ensure that the harvested mushrooms are suitable for the fresh market. The WI value helps assess the quality of mushrooms post-harvest, providing insight into how well the end-effector preserves the mushroom's appearance.

After harvesting, the WI for mushrooms from each treatment were measured. Table 2 compares the WI values across different treatments immediately after harvest (day 0). An ANOVA test revealed a significant difference among the treatments (p-value < 0.001). To evaluate the impact of different harvesting pressures on the WI, a Fisher's pairwise comparison at a 95% confidence level was performed. The results indicate that one of the treatments belongs to the same group as another, implying no significant difference in the WI values.

The analysis revealed that mushrooms could be categorized into three groups based on WI values: Group A (-5 kPa), Group B (hand-picking, -10 kPa, and -15 kPa), and Group C (-20 kPa). The 95% confidence interval plot in Figure 22 illustrates that mushrooms harvested at -5 kPa exhibited the highest WI, indicating superior quality, whereas those harvested at -20 kPa had the lowest. The remaining treatments, including hand-picking and the pressures of -10 kPa and -15 kPa, showed no significant difference in the mean WI.

Table 2. Grouping information using the Fisher's LSD method and 95% confidence (After harvest Day 0).

Factor	N	Mean	Standard Deviation	Grouping	
Hand Picking	50	43.07	2.97	B	
-5kPa	50	44.38	3.09	A	
-10kPa	50	42.88	2.12	B	
-15kPa	50	42.78	2.14	B	
-20kPa	50	39.79	3.29		C

Means that not share a letter are significantly different

 doi:10.20944/preprints202602.0774.v1

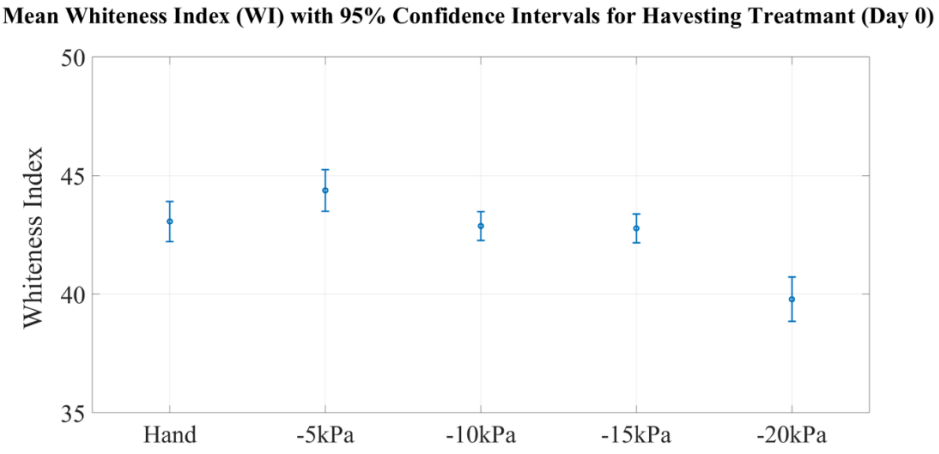

Figure 22. Comparison of Whiteness Index (WI) with 95% confidence intervals across different harvesting methods. Mushrooms harvested at −5 kPa exhibited the highest WI, while those harvested at −20 kPa showed the lowest. No significant differences were observed among the hand-picked, −10 kPa, and −15 kPa treatments.

The quality of fresh white button mushrooms was evaluated by measuring the decrease in the whiteness index over an eight-day storage period. Figure 23 provides an example of the data collected, showing images of mushrooms harvested by hand and under vacuum pressures of -5, -10, -15, and -20 kPa. Images were taken every 24 hours, starting 2 hours after harvest on day 0 and continuing until day 8. The images visually demonstrate the natural and gradual browning process of the mushrooms over time across different harvesting methods.

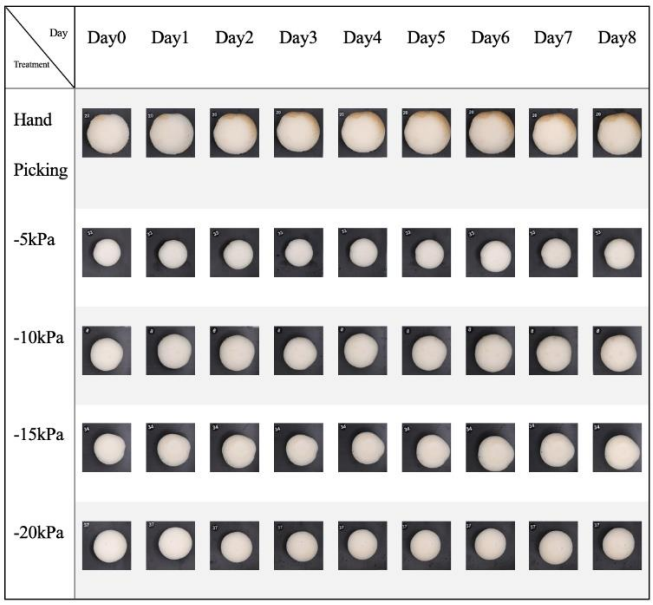

Figure 23. Time-series images of white button mushrooms harvested by hand and using vacuum pressures of –5, –10, –15, and –20 kPa, captured over an eight-day storage period. Photographs were taken every 24 hours beginning 2 hours post-harvest (Day 0) through Day 8. The images illustrate the gradual browning process and visual quality changes associated with each harvesting method.

Figure 24 illustrates the kinetics of the average WI for different harvest treatments over time. The appearance of the mushroom cap, the first aspect consumers notice, plays a crucial role in determining shelf life. The WI generally decreases over time, reflecting the mushrooms' natural aging and browning process.

 doi:10.20944/preprints202602.0774.v1

As shown in Table 3, an ANOVA test conducted on the final day revealed statistically significant differences among the treatments (p-value < 0.001) with 95% confidence. Fisher's LSD post-hoc analysis further identified three distinct groups based on WI. The treatments involving -5, -10, and -15 kPa vacuum pressures were grouped, sharing similar mean WI values. In contrast, hand-picked mushrooms formed a separate group, while the mushrooms harvested with -20 kPa vacuum pressure had the lowest WI and constituted the last group.

Table 3. Grouping information using the Fisher's LSD method and 95% confidence (After harvest Day 8).

Factor	N	Mean	Standard Deviation	Grouping		
Hand Picking	50	34.05	6.73	A		
-5kPa	50	36.71	4.03		B	
-10kPa	50	37.74	3.78		B	
-15kPa	50	38.22	3.97		B	
-20kPa	50	28.72	6.89			C

Means that not share a letter are significantly different

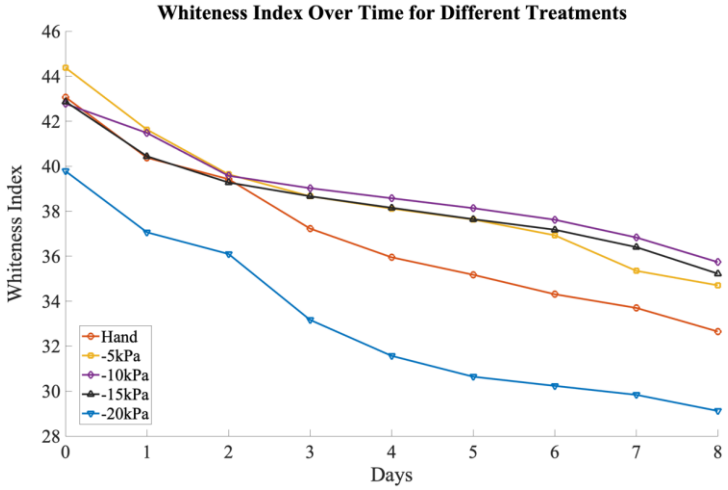

Figure 24. Kinetics of the average WI over time.

3.7. Recommended Pressure

A contour plot, as shown in Figure 24, was utilized to determine the recommended vacuum pressure for harvesting mushrooms with this specific end-effector design. This plot visualizes pressure as a function of the success rate and the resulting WI (Day 0), allowing us to identify the pressure that maximizes these two critical factors. The analysis determined the recommended vacuum pressure as -17.17 kPa, where mushrooms maintain the highest quality, as indicated by their WI, while achieving a high success rate during harvesting. This pressure is recommended for use with the current end-effector design to ensure optimal harvesting performance.

 doi:10.20944/preprints202602.0774.v1

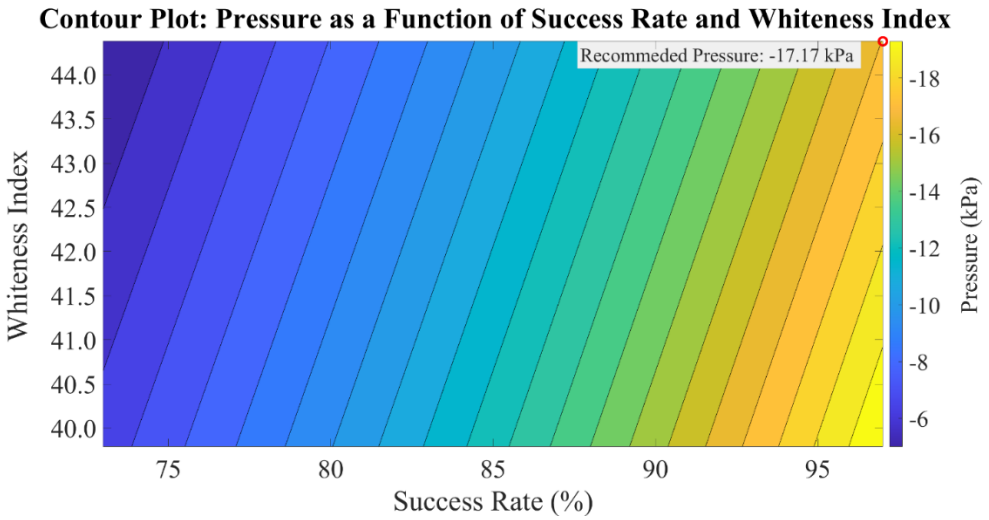

Figure 25. Contour plot for recommended vacuum pressure.

The vacuum cup has the advantage of approaching the top of the mushroom and picking it up efficiently. However, any damage caused by the vacuum cup on the mushroom cap can negatively impact the market value, particularly for those intended for the fresh market, where appearance is critical. This potential impact on market value underscores the importance of this research.

The observations revealed that mushrooms picked with the vacuum cup did not show any visible damage to the cap 2 hours (day 0) after harvest or even after eight days of storage. This suggests that if the vacuum cup does not cause visible damage immediately after harvest, such damage is unlikely to appear later. However, if the vacuum cup does leave damage on the mushroom cap, this damage becomes more apparent over time as the mushroom continues to brown due to the natural aging process, underscoring the need for caution in the use of vacuum cups.

Figure 25 provides an example of mushrooms harvested with a vacuum pressure of -15 kPa. Without any initial damage on the cap, the mushroom continued to brown uniformly over time, which is a natural process (top row). In contrast, the mushroom that sustained damage from the vacuum cup exhibited more noticeable browning at the damaged site, making the damage more apparent as time progressed (bottom row).

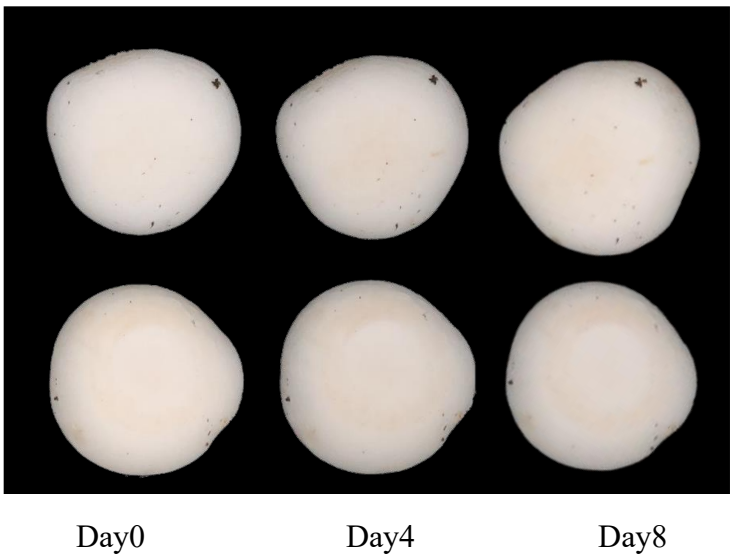

Figure 26. Comparison of mushroom browning over time at -15 kPa vacuum pressure.

These findings highlight a crucial consideration for the design of end-effectors that utilize vacuum cups for mushroom harvesting. Ensuring that the vacuum cup does not cause immediate

 doi:10.20944/preprints202602.0774.v1

visible damage to the mushroom cap is essential for maintaining the mushroom's quality and marketability in the fresh market. If the cap remains undamaged after harvest, the mushroom will likely continue to age naturally without developing additional visible defects, making it suitable for sale in the fresh produce market.

The end-effector developed demonstrated that high vacuum pressure can achieve a high success rate in harvesting mushrooms; however, it is essential to balance this with the potential risk of damaging the mushroom cap, which could negatively impact marketability. This study highlights three critical considerations to optimize the harvesting process while minimizing damage. First, the material of the vacuum cup is crucial, as the friction coefficient between the cup and the mushroom determines the effectiveness of the grip. Selecting a material with the appropriate friction properties ensures successful harvesting without causing harm. Second, the design of the vacuum cup plays a significant role; a simple design was utilized with a single vacuum cup, and the surface area of the sealing lip is critical in determining the holding force. Increasing the contact area can enhance the success rate while reducing the risk of damage. Ensuring the vacuum pressure is optimal is essential for maintaining the mushroom's quality, especially for the fresh market.

Additionally, the study focused on the mechanism of picking mushrooms that grow close to each other, where the bending angle becomes a crucial factor. The end-effector must avoid bending the mushroom toward surrounding mushrooms, as contact between them can cause the vacuum cup to leak and fail to pick the mushroom. Instead, the end-effector should bend the mushroom into the available space for picking. Furthermore, the stem-cutting mechanism must be carefully managed to avoid breaking the mushroom stem, which could lead to bruising. While the duration for which the vacuum cup holds the mushroom after picking was controlled, future research should consider developing an automated system to optimize the stem-cutting process further. By addressing these factors, the design of end-effectors using vacuum cups can be refined to improve the efficiency and effectiveness of mushroom harvesting, ensuring a high success rate and preserving mushroom quality.

4. Conclusions

The end-effector, designed to mimic manual harvesting, was developed to bend and twist white button mushrooms using a vacuum-based mechanism. A comprehensive analysis of the friction coefficient between the mushroom surface and the silicone vacuum cup, along with the forces and torques involved in bending and twisting, identified vital parameters that directly impact the efficiency and quality of the harvesting process.

The friction coefficient, with a mean value of 0.62, was crucial in ensuring a secure grip while minimizing damage to the mushroom cap. The findings underscore the importance of calibrating vacuum pressure based on the friction coefficient to optimize the balance between grip strength and mushroom integrity.

The critical bending angle averaged 5.72°, while the torque required for twisting averaged 2.56 Nm. These parameters were used to determine the minimum vacuum pressures needed for effective harvesting: -8.64 kPa (±2.21) for bending and -8.91 kPa (±2.45) for twisting. A p-value of 0.514 indicated no significant difference between the pressures required for bending and twisting. The end-effector's ability to bend the mushroom at 10° and twist it 90° was validated by the bending and twisting tests. The recommended vacuum pressure of -17.17 kPa was identified, providing a high success rate while preserving mushroom quality, as measured by the WI.

It is crucial to carefully consider the design and operation of the end-effector. The material and lip area of the vacuum cup, the direction of mushroom bending, and the duration of vacuum application are all key factors that influence the outcome of the harvesting process. By optimizing these elements, the risk of damage can be significantly reduced, improving the marketability of the harvested mushrooms.

This research provides valuable insights into the design and operation of vacuum-based end-effectors for mushroom harvesting, demonstrating that robotic harvesting can effectively serve the

 doi:10.20944/preprints202602.0774.v1

fresh market. By addressing the identified factors, future developments can enhance the efficiency and effectiveness of these systems, ensuring a high success rate in mushroom harvesting while preserving the quality required for the fresh market. These findings contribute to the field, guiding future research and development in mushroom harvesting technology.

Author Contributions: Conceptualization, K.P., L.H., and Y.Y.; methodology, K.P.; software, K.P. and Y.Y.; validation, K.P. and Y.Y.; formal analysis, K.P.; investigation, K.P.; resources, Y.Y., L.H., and J.P.; data curation, K.P. and Y.Y.; writing—original draft preparation, K.P.; writing—review and editing, K.P., Y.Y., L.H., J.P., and P.H.; visualization, K.P.; supervision, L.H., P.H.; project administration, L.H. and J.P.; funding acquisition, L.H., J.P., and Y.Y. All authors have read and agreed to the published version of the manuscript.

Funding: This research was partially supported by the United States Department of Agriculture, National Institute of Food and Agriculture (USDA NIFA), Federal Appropriations under Project PEN04822 and Accession No. 7005925. This work was also supported by the USDA National Institute of Food and Agriculture Specialty Crop Research Initiative (SCRI) under Grant No. 2021-51181-35859. The APC was funded by the University of Tennessee Institute of Agriculture.

Data Availability Statement: The data presented in this study are available upon reasonable request.

Acknowledgments: The authors would like to thank the staff and technicians at the Penn State Mushroom Research Center (MRC) for their assistance with mushroom cultivation and for maintaining the experimental facilities throughout the study.

Conflicts of Interest: The authors declare no conflicts of interest.

Abbreviations

The following abbreviations are used in this manuscript:

Symbol	Description	Unit
Ao	Area of the outer circle of the vacuum cup	m^2
Ai	Area of the inner circle of the vacuum cup	m^2
Do	Diameter of the outer lip of the vacuum cup	m
Di	Diameter of the inner lip of the vacuum cup	m
F	Vacuum-generated force during bending	N
Fs	Vacuum-generated force during bending	N
f	Frictional force resisting relative motion	N
H	Vertical distance from contact point to mushroom bottom	m
Mt	Total torque exerted during twisting	Nm
Pvacuum	Vacuum pressure required for harvesting	Pa
Patm	Atmospheric pressure	Pa
Psuction	Suction pressure inside the vacuum cup	Pa
r	Distance from pivot point to force application point	m
r1	Inner radius of vacuum cup contact area	m
r2	Outer radius of vacuum cup contact area	m
X	Horizontal displacement during bending	m
α	Bending angle	degrees (°)
μ	Friction coefficient between vacuum cup and mushroom cap	-
WI	Whiteness Index (indicator of mushroom color quality)	-
$L*$	Lightness component in the CIELAB color space	-
$a*$	Red–green chromaticity component in CIELAB	-
$b*$	Yellow–blue chromaticity component in CIELAB	-

References

1. Alston, J. M. & Pardey, P. G. *Public Funding for Research into Specialty Crops*. *HORTSCIENCE* vol. 43 http://www.ers.usda.gov/data/FarmIncome/; (2008).

 doi:10.20944/preprints202602.0774.v1

2. USDA-NASS. Mushroom annual report. Washington, D.C.: USDA National Agricultural Statistic Service (2023).
3. Valverde, J. Harvesting and Processing of Mushrooms. in *Edible and Medicinal Mushrooms* 261–270 (2017). doi:https://doi.org/10.1002/9781119149446.ch13.
4. Azoyan, A. Feasibility analysis of an automated mushroom harvesting system. (2004).
5. Koirala, B. et al. Robotic Button Mushroom Harvesting Systems: A Review of Design, Mechanism, and Future Directions. *Applied Sciences* **14**, 9229 (2024).
6. Reed, J. N. & Tillett, R. D. Initial experiments in robotic mushroom harvesting. *Mechatronics* **4**, 265–279 (1994).
7. Noble, R., Reed, J. N., Miles, S., Jackson, A. F. & Butler, J. Influence of Mushroom Strains and Population Density on the Performance of a Robotic Harvester. *Journal of Agricultural Engineering Research* **68**, 215–222 (1997).
8. Reed, J. N., Miles, S. J., Butler, J., Baldwin, M. & Noble, R. Automatic mushroom harvester development. *Journal of Agricultural and Engineering Research* **78**, 15–23 (2001).
9. Noble, R., Reed, J. N., Miles, S., Jackson, A. F. & Butler, J. Influence of Mushroom Strains and Population Density on the Performance of a Robotic Harvester. *Journal of Agricultural Engineering Research* **68**, 215–222 (1997).
10. Tillett, R. D. & Batchelor, B. G. An algorithm for locating mushrooms in a growing bed. *Comput. Electron. Agric.* **6**, 191–200 (1991).
11. Yang, S., Ni, B., Du, W. & Yu, T. Research on an Improved Segmentation Recognition Algorithm of Overlapping Agaricus bisporus. *Sensors* **22**, 3946 (2022).
12. Chen, C., Wang, F., Cai, Y., Yi, S. & Zhang, B. An Improved YOLOv5s-Based Agaricus bisporus Detection Algorithm. *Agronomy* **13**, 1871 (2023).
13. Retsinas, G., Efthymiou, N., Anagnostopoulou, D. & Maragos, P. Mushroom Detection and Three Dimensional Pose Estimation from Multi-View Point Clouds. *Sensors* **23**, 3576 (2023).
14. Wei, B. et al. Recursive-YOLOv5 Network for Edible Mushroom Detection in Scenes With Vertical Stick Placement. *IEEE Access* **10**, 40093–40108 (2022).
15. Dai, Y., Xiang, C., Qu, W. & Zhang, Q. A Review of End-Effector Research Based on Compliance Control. *Machines* **10**, 100 (2022).
16. Koirala, B. et al. A Hybrid Three-Finger Gripper for Automated Harvesting of Button Mushrooms. *Actuators* **13**, 287 (2024).
17. Huang, M., He, L., Choi, D., Pecchia, J. & Li, Y. Picking dynamic analysis for robotic harvesting of Agaricus bisporus mushrooms. *Comput. Electron. Agric.* **185**, 106145 (2021).
18. Yang, S., Ji, J., Cai, H. & Chen, H. Modeling and Force Analysis of a Harvesting Robot for Button Mushrooms. *IEEE Access* **10**, 78519–78526 (2022).
19. Zhao, K. et al. Pressure-Stabilized Flexible End-Effector for Selective Picking of Agaricus bisporus. *Agriculture* **13**, 2256 (2023).
20. Fantoni, G. et al. Grasping devices and methods in automated production processes. *CIRP Annals* **63**, 679–701 (2014).
21. Mbakop, S., Tagne, G., Lagache, A., Youcef-Toumi, K. & Merzouki, R. Integrated design of a bio-inspired soft gripper for mushrooms harvesting. in *2023 IEEE International Conference on Soft Robotics (RoboSoft)* 1–6 (IEEE, 2023). doi:10.1109/RoboSoft55895.2023.10122042.
22. Recchia, A. et al. A Prototype Pick and Place Solution for Harvesting White Button Mushrooms Using a Collaborative Robot. *Robotics Reports* **1**, 67–81 (2023).
23. Galley, A., Knopf, G. K. & Kashkoush, M. Pneumatic Hyperelastic Actuators for Grasping Curved Organic Objects. *Actuators* **8**, 76 (2019).
24. Tao, K., Wang, Z., Yuan, J. & Liu, X. Design of a novel end-effector for robotic bud thinning of Agaricus bisporus mushrooms. *Comput. Electron. Agric.* **210**, 107880 (2023).
25. Galley, A., Knopf, G. K. & Kashkoush, M. Pneumatic Hyperelastic Actuators for Grasping Curved Organic Objects. *Actuators* **8**, 76 (2019).

 doi:10.20944/preprints202602.0774.v1

26. Burton, K. Cultural factors affecting mushroom quality – causes and control of bruising. *Mushroom Science* **16**, 397–402 (2004).
27. Burton Ks, R. T. Brusing: a market effect. *Mushroom Journal* **617**, 20–22 (2001).
28. Burton KS. Brusing means lost mushroom sales. *Mushroom Journal* **624**, 23–24 (2002).
29. Weijn, A. et al. A new method to apply and quantify bruising sensitivity of button mushrooms. *Food Sci. Technol. Res.* **47**, 308–314 (2012).
30. Huang, M. et al. Development of a Robotic Harvesting Mechanism for Button Mushrooms. *Trans. ASABE* **64**, 565–575 (2021).
31. Esposito, A. *Fluid Power with Applications*. (Pearson Prentice Hall, 2009).
32. Monkman, G. J., Hesse, S., Steinmann, R. & Schunk, H. *Robot Grippers*. (Wiley, 2007).
33. Slosson, J. C. & Yi, H. Characterization of mechanical biomass particle-particle and particle-wall interactions. Preprint at (2025).